Article

TRANSPARENT PROCESS

THE EMBO JOURNAL

Cytosolic RNA:DNA hybrids activate the cGAS–STING axis

Arun K Mankan[1], Tobias Schmidt[1,†], Dhruv Chauhan[1,†], Marion Goldeck[2], Klara Höning[1], Moritz Gaidt[1], Andrew V Kubarenko[1,‡], Liudmila Andreeva[3], Karl-Peter Hopfner[3] & Veit Hornung[1,*]

Abstract

Intracellular recognition of non-self and also self-nucleic acids can result in the initiation of potent pro-inflammatory and antiviral cytokine responses. Most recently, cGAS was shown to be critical for the recognition of cytoplasmic dsDNA. Binding of dsDNA to cGAS results in the synthesis of cGAMP(2′–5′), which then binds to the endoplasmic reticulum resident protein STING. This initiates a signaling cascade that triggers the induction of an antiviral immune response. While most studies on intracellular nucleic acids have focused on dsRNA or dsDNA, it has remained unexplored whether cytosolic RNA:DNA hybrids are also sensed by the innate immune system. Studying synthetic RNA:DNA hybrids, we indeed observed a strong type I interferon response upon cytosolic delivery of this class of molecule. Studies in THP-1 knockout cells revealed that the recognition of RNA:DNA hybrids is completely attributable to the cGAS–STING pathway. Moreover, *in vitro* studies showed that recombinant cGAS produced cGAMP upon RNA:DNA hybrid recognition. Altogether, our results introduce RNA:DNA hybrids as a novel class of intracellular PAMP molecules and describe an alternative cGAS ligand next to dsDNA.

Keywords cGAS; innate immunity; pattern recognition receptor; RNA:DNA hybrids; STING

Subject Categories Immunology; Microbiology, Virology & Host Pathogen Interaction

DOI 10.15252/embj.201488726 | Received 14 April 2014 | Revised 14 October 2014 | Accepted 24 October 2014 | Published online 25 November 2014

The EMBO Journal (2014) 33: 2937–2946

Introduction

The innate immune system has evolved to defend the host against invading pathogens. An important prerequisite for this task is the specific and reliable detection of different microbial pathogens as non-self. This is achieved by a conserved set of germ-line-encoded pathogen recognition receptors (PRRs) that have evolved to detect so-called pathogen-associated molecular patterns (PAMPs) as foreign. PRRs include, amongst others, Toll-like receptors (TLRs), Nod-like receptors (NLRs) and RIG-I-like receptors (RLRs) (Medzhitov, 2007).

Detection of virus-derived nucleic acids plays a central role in the initiation of antiviral immunity. Nucleic acid recognition by PRRs results in the secretion of type I interferon (IFN) cytokines and IFN-stimulated genes (ISGs), which function to impede viral replication. For example, 5′-triphosphorylated RNA is detected by the cytoplasmic RNA helicase RIG-I, whereas long double-stranded RNA is sensed by its related family member MDA5. Both RIG-I and MDA5 signal via their shared signaling adapter molecule MAVS, located at the mitochondrion (Goubau *et al*, 2013). In certain cell types, RNA can also be detected by TLR7 and TLR8, located in the endolysosomal compartment. While these receptors display a certain preference for non-self RNA, they are in principle also responsive to endogenous RNA molecules. However, under normal circumstances, their localization in the endolysosomal compartment shields them from endogenous RNA molecules, thereby precluding erroneous activation by self-molecules. A similar scenario holds true for TLR9, which is also located in the endolysosome, detecting DNA of certain sequence composition (CpG motifs) (Barbalat *et al*, 2011). More recently, a cytosolic nucleotidyltransferase named cGAS (cyclic GMP-AMP synthase) was identified as the key sensor required for DNA recognition in the cytoplasm (Sun *et al*, 2013; Wu *et al*, 2013). Upon binding to dsDNA, cGAS catalyzes the formation of the cyclic dinucleotide (CDN) molecule cGAMP using ATP and GTP as substrates. Unlike previously known prokaryotic CDNs, the cGAS-derived CDN contains an unusual 2′–5′ phosphodiester linkage between GMP and AMP, with its second phosphodiester linkage being 3′–5′: >Gp(2′–5′)Ap(3′–5′)>(cGAMP(2′–5′)) (Ablasser *et al*, 2013a; Diner *et al*, 2013; Gao *et al*, 2013b; Wu *et al*, 2013; Zhang *et al*, 2013). Upon formation, cGAMP(2′–5′) binds to the endoplasmic reticulum resident protein STING, which results in the activation of the TBK1/IRF3 pathway and as such the production of type I interferons. Interestingly, cGAMP(2′–5′) is not only bound to exert its antiviral activity within the cell it has been produced in, but it can also be passed on to bystander cells via gap junctions. This, in

1 Institute of Molecular Medicine, University Hospital, University of Bonn, Bonn, Germany
2 Institute of Clinical Chemistry and Clinical Pharmacology, University Hospital, University of Bonn, Bonn, Germany
3 Department of Biochemistry and Gene Center, Ludwig-Maximilians-University, Munich, Germany
*Corresponding author. Tel: +49 228 287 51203; Fax: +49 228 287 51201; E-mail: veit.hornung@uni-bonn.de
†These authors contributed equally
‡Present address: Institute of Clinical Chemistry and Clinical Pharmacology, University Hospital, University of Bonn, Bonn, Germany

turn, can then initiate antiviral immune responses in cells that have not been in contact with a virus yet (Ablasser *et al*, 2013c).

As mentioned above, certain PRRs not only recognize pathogenic components but can also sense self-molecules, once mislocalized in the respective PRR compartment (Ablasser *et al*, 2013b). For example, defects in cytoplasmic nucleases can result in the accumulation of endogenous nucleic acids in the cytosol and thereby lead to the activation of innate sensing pathways. Aicardi–Goutières syndrome (AGS) is a rare but generally fatal childhood inflammatory condition with neurological dysfunction, that is associated with increased production of type I interferons (Crow, 2011; Lee-Kirsch *et al*, 2014). This disease predominantly results from loss-of-function mutations in nucleic acid metabolizing enzymes such as SAMHD1, TREX1, Ribonuclease H2 (RNASE H2A, RNASE H2B, RNASE H2C) or ADAR1 (Gall *et al*, 2012; Lee-Kirsch *et al*, 2014). TREX1 deficiency in mice has been shown to result in the accumulation of endogenous DNA molecules, which can serve as ligands for the cGAS–STING axis and as such initiate antiviral immunity (Gall *et al*, 2012; Ablasser *et al*, 2014). However, the exact nature of these ligands is currently not known. On the other hand, ablation of the *Rnaseh2b* gene in mice results in the incorporation of ribonucleotides in the genomic DNA; however, a mechanistic link to PRR-mediated proinflammatory gene expression has not been established (Reijns *et al*, 2012).

Intrigued by the possibility of cytosolic RNA:DNA hybrids serving as PAMP molecules on their own, we set forth to investigate the immunostimulatory capacity of this class of molecules in cells competent for both dsRNA and dsDNA sensing pathways.

Results

Intracellular RNA:DNA hybrids induce antiviral gene expression

Using *in vitro* transcribed RNA molecules (e.g. T7 RNA polymerase) as templates for reverse transcriptase, RNA:DNA hybrids of different lengths can easily be produced enzymatically. However, reverse transcriptase also possesses DNA-dependent DNA polymerase activity and as such can generate dsDNA from the newly synthesized ssDNA (Hsieh *et al*, 1993). Therefore, to faithfully exclude dsDNA contamination in assessing the immunostimulatory capacity of DNA:RNA hybrids, we made use of enzymatically generated homopolymers of poly(rA) and poly(dT). Annealing of poly(rA) and poly (dT) resulted in the formation of a poly(rA):poly(dT) RNA:DNA hybrid with a predominant band of around 1,300 bp (Fig 1A). To confirm that this product indeed represented a RNA:DNA hybrid, we performed dot-blot assays wherein membrane-immobilized nucleic acids were probed with a monoclonal antibody (S9.6) specific for RNA:DNA hybrids (Boguslawski *et al*, 1986; Hu *et al*, 2006). We observed a specific detection of the hybrid by the antibody, correlating with the amount of nucleic acids immobilized (Fig 1B). Digestion of the hybrid with RNase A which digests dsRNA, DNase I which digests dsDNA or ssDNA and RNase H which digests RNA part of RNA:DNA hybrids provided further confirmation regarding the purity of the hybrid. Thus, while the RNA:DNA hybrid was completely digested by RNase H and DNase I enzymes, it was resistant, as expected, to RNase A activity (Fig 1C). Control experiments confirmed the specificity of these enzymes on dsDNA or dsRNA, respectively (A.K. Mankan, unpublished observations). In order to assess the biological activity of RNA:DNA hybrids, we then transfected the poly(rA):poly(dT) hybrids or the single components poly(rA) or poly(dT) into murine bone marrow-derived macrophages. Transfection of the hybrids resulted in a robust induction of type I IFNs and pro-inflammatory genes (*Ifna*, *Ifnb*, *Il6* and *Ip10)* (Supplementary Fig S1A). Of note, a significant activity of poly(dT), by itself, was also observed for some readouts studied (see discussion below). To assess the relevance of hybrids in the human system, we next transfected hybrids or the individual polynucleotide components into peripheral blood mononuclear cells. RT–PCR confirmed enhanced expression of *IFNB* gene in PBMCs transfected with hybrids (Fig 1D). Synthetic poly(dA):poly (dT), which was transfected as a dsDNA control, showed higher activity with regard to *IFNB* induction. We also observed a significant secretion of IP-10 in response to the RNA:DNA hybrids, while only a minimal IP-10 induction was seen in cells transfected with the single polynucleotides (Fig 1E). We next tested the activity of RNA:DNA hybrids in differentiated human THP-1 cells. In line with the PBMC data, RNA:DNA hybrids induced robust transcription of *IFNB* in THP-1 cells, again with dsDNA being more active (Fig 1F). In order to have a sensitive readout for antiviral gene expression, we equipped THP-1 cells with Gaussia luciferase (GLuc) under the promoter of *IFIT1*, a well-characterized ISG that is also directly transcribed upon PRR stimulation (Supplementary Fig S2A). Studying pIFIT1-GLuc THP-1 in response to these different stimuli paralleled the data obtained by measuring *IFNB* (Fig 1G). However, as observed in the previous set of experiments, the transactivation of the *IFIT1* promoter in response to RNA:DNA hybrid was never as strong as upon dsDNA transfection, also when compared over a broad range of different ligand concentrations (Fig 1H). Interestingly, assessing the production of the antiviral chemokine IP-10 in response to these stimuli revealed a similar plateau for both hybrids as well as dsDNA at higher ligand concentrations, most likely due to the fact that this chemokine is induced by both PRR-dependent as well as type I IFN-dependent mechanisms (Supplementary Fig S1B). Altogether, these data indicated that intracellular RNA:DNA hybrids are indeed sensed by the innate immune system, leading to strong antiviral immune responses.

RNA:DNA hybrid detection is independent of MAVS but requires the cGAS–STING axis

We next focused on the identification of the intracellular receptor that was essential for mediating the RNA:DNA hybrid-induced innate immune response. As RNA:DNA hybrids contain a single polyribonucleotide molecule, we first assessed the involvement of the RLR system as sensors of RNA-DNA hybrids. MAVS constitutes the critical signaling adapter downstream of both RIG-I and MDA-5 and as such, MAVS-deficient cells are devoid of both RIG-I and MDA5 signaling. We made use of the CRISPR/Cas9 gene editing system to knock out MAVS in THP-1 cells. As such, we targeted a critical coding exon to disrupt the reading frame and therefore the expression of MAVS (Supplementary Fig S2B). Transfection of differentiated wild-type (WT) THP-1 cells with RNA:DNA hybrids resulted in increased *IFNB,* and a similar response was also observed in *MAVS* knockout cells (Fig 2A). As expected, MAVS-deficient THP-1 cells failed to respond to 5′-triphosphate RNA, whereas dsDNA-mediated activation of THP-1 cells was not affected.

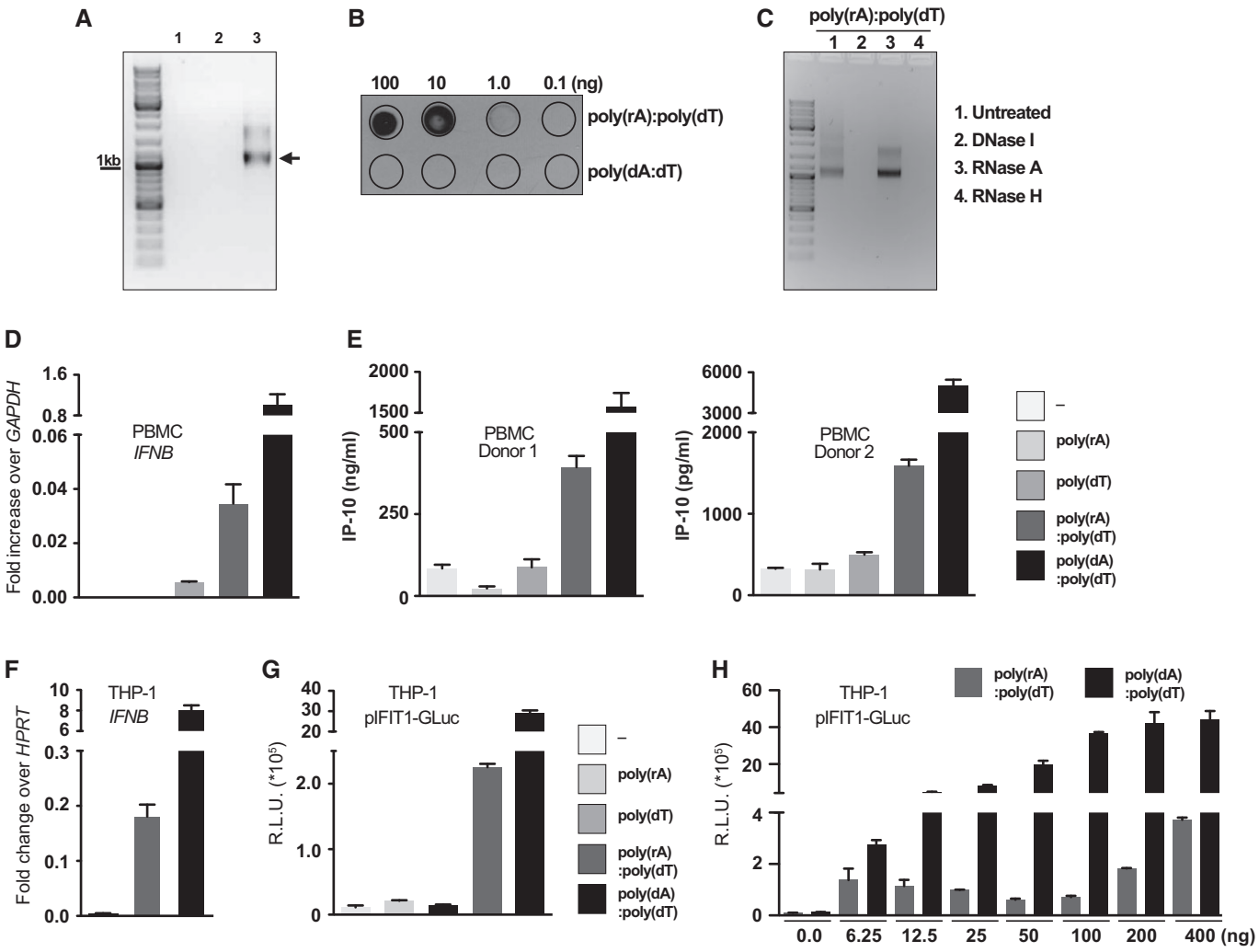

Figure 1. Synthetic annealed poly(rA):poly(dT) hybrid induces type I interferon response.

A Synthetic poly(rA) (lane 1) and poly(dT) (lane 2) oligos were annealed, and the samples were run on a 1% agarose gel. Arrows indicate the annealed poly(rA):poly(dT) (lane 3) RNA:DNA hybrid.

B Different amounts of synthetic annealed poly(rA):poly(dT) hybrid was spotted on a nitrocellulose membrane and probed with anti-hybrid S9.6 antibody.

C Poly(rA):poly(dT) was either undigested (1) or digested with DNase I (2), RNase A (3) or RNase H (4), and the digested samples were analyzed on a 1% agarose gel.

D Human peripheral blood mononuclear cells (PBMCs) were transfected with or without poly(rA), poly(dT) or poly(rA):poly(dT) hybrid or poly(dA):poly(dT) dsDNA for 6 h. RT–PCR was performed to check for the expression of *IFNB*. Figure shows values from two biological replicates. Data plot shows mean with SEM.

E Human PBMCs from two different donors were transfected with or without poly(rA), poly(dT) or poly(rA):poly(dT) for 16 h, and the amount of secreted IP-10 was measured by ELISA. Each experiment was performed in duplicate. Data plot shows mean with SEM.

F Differentiated human monocyte THP-1 cells were transfected with or without poly(rA):poly(dT) hybrid, poly(dA):poly(dT) dsDNA and RT–PCR was performed to check for the expression of *IFNB*. Each experiment was performed in duplicate. Data are representative of one of two independent experiments. Data plot shows mean with SEM.

G Differentiated human monocyte THP-1 cells with Gaussia luciferase knockin under *IFIT1* promoter were transfected with or without poly(rA):poly(dT) hybrid, poly(dA):poly(dT) dsDNA and luciferase assay was performed. Data shown are from two biological replicates. Data plot shows mean with SEM.

H Differentiated human monocyte THP-1 cells with Gaussia luciferase knockin under *IFIT1* promoter were transfected with different amounts of poly(rA):poly(dT) hybrid or poly(dA):poly(dT) dsDNA and luciferase assay was performed. Data shown are from two biological replicates. Data plot shows mean with SEM.

To study the involvement of the cGAS–STING axis in RNA:DNA hybrid recognition, we next generated THP-1 cells deficient in either STING or cGAS (Supplementary Fig S2C and D). Interestingly, we did not observe any induction of *IFNB* in response to transfection of RNA:DNA hybrids in differentiated *STING* or *cGAS* KO THP-1 cells (Fig 2B–D). As anticipated, dsDNA-mediated *IFNB* induction was also completely abrogated in *cGAS/STING* KO cells, whereas 5′-triphosphate RNA detection was still intact. Similar results were also observed for IL-6 (Supplementary Fig S3). These data suggested that, next to dsDNA, cGAS also serves as the receptor for cytosolic RNA:DNA hybrids.

RNA:DNA hybrids bind with cGAS and produce cGAMP

To confirm the direct recognition of RNA:DNA hybrids by cGAS, we took advantage of the fact that cGAS-mediated activation can be

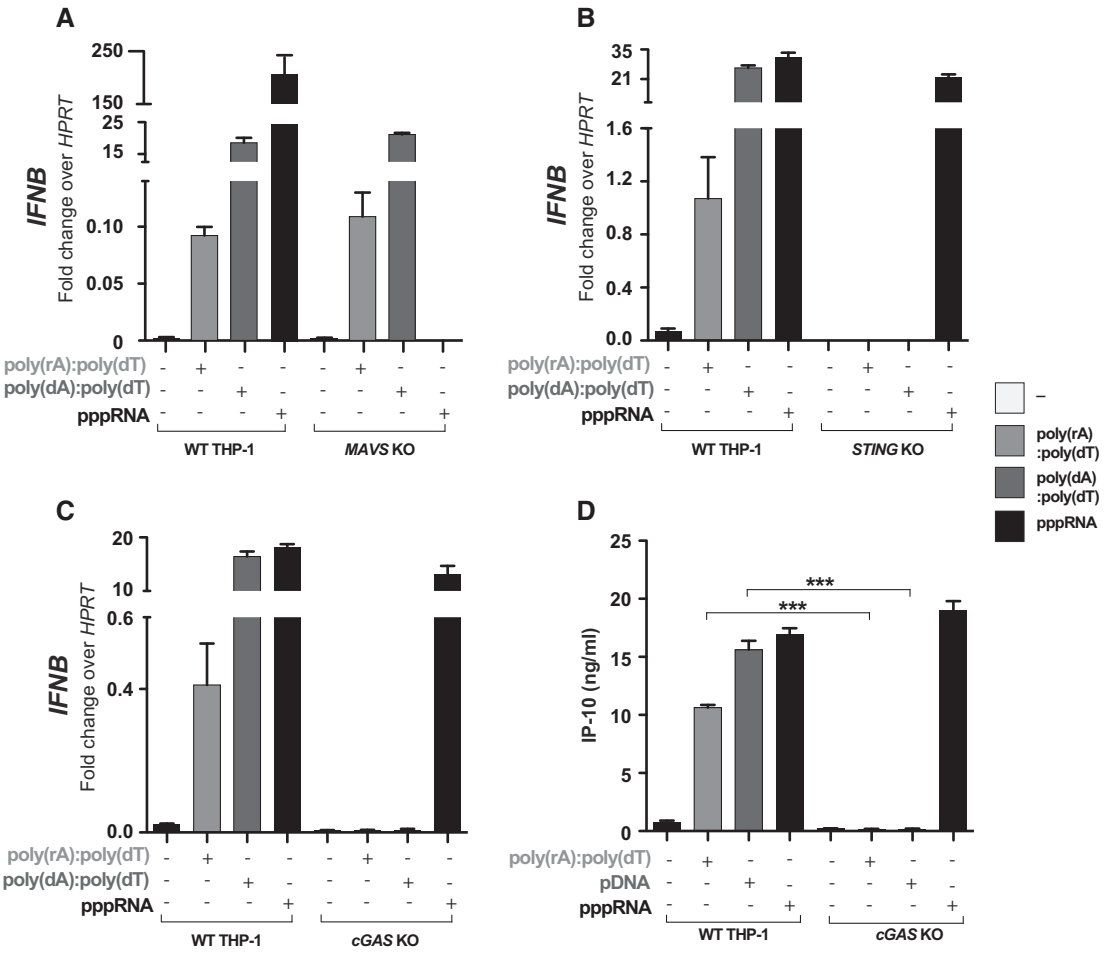

Figure 2. Poly(rA):poly(dT) RNA:DNA hybrids-induced type I interferon response is cGAS dependent.

A–C WT THP-1, *MAVS* KO THP-1, *STING* KO THP-1 and *cGAS* KO THP-1 cells were transfected with or without poly(rA):poly(dT) (hybrid), poly(dA):poly(dT) dsDNA or pppRNA for 6 h. RT–PCR was performed to check for the expression of *IFNB*. Data shown are from experimental duplicates representative of two independent experiments. Data plot shows mean with SEM.

D WT THP-1 cells or *cGAS* KO THP-1 cells were transfected with or without poly(rA):poly(dT) (hybrid), dsDNA or pppRNA for 16 h, and amount of IP-10 secreted was detected by ELISA. Data shown are from experimental triplicate, representative of three independent experiments. Data plot shows mean with SEM.

Data information: ***$P < 0.0001$, one-way ANOVA, Tukey's multiple comparison test.

studied *in vitro*. To this effect, we incubated the single polynucleotides (poly(rA) and poly(dT)) or the synthetic RNA:DNA hybrids (poly(rA):poly(dT)) with recombinant cGAS in the presence of ATP and GTP. Moreover, we included synthetic dsRNA (poly(rA):poly(rU)) and synthetic dsDNA (poly(dA):poly(dT)) as controls. The samples were incubated for 45, 90 or 180 min. Analysis of the RNA:DNA/cGAS sample via HPLC revealed a peak correlating with the expected peak for cGAMP(2′–5′) (Fig 3A). However, no such product was observed upon the incubation of cGAS with dsRNA or any of the single polynucleotide preparations (Fig 3C and Supplementary Fig S4A). Compared to dsDNA, RNA:DNA hybrids induced less cGAMP, also when studying cGAMP production over time (Supplementary Fig S4B). Several groups have recently used shorter length synthetic ssRNA and ssDNA to generate hybrids and to study the immune cell activation by these shorter hybrids. To confirm whether such short hybrids can also activate cGAS–cGAMP pathway, we used 60-bp synthetic poly(rA) ssRNA and poly(dT) ssDNA oligos and generated RNA:DNA hybrids by annealing them (Fig 4A). To verify whether these shorter oligos were functionally active, we transfected them into pIFIT1-GLuc THP-1 cells and observed a robust secretion of luciferase only in response to hybrids and dsDNA (Fig 4B). As above, incubation of these shorter hybrids with recombinant cGAS clearly resulted in the formation of cGAMP (Fig 4C).

To understand the structural basis for the interaction of cGAS with RNA:DNA hybrids, we generated protein–nucleic acid interaction models *in silico*. Modeling of the complexes of cGAS with either RNA:DNA hybrid, dsDNA or dsRNA revealed that RNA:DNA hybrid could bind in the cleft of cGAS (regardless of the orientation of RNA and DNA strands) exactly in the same mode as dsDNA. At the same time, the dsRNA helix could not be accommodated in this cleft (Fig 5A–D). Structural alignment of dsDNA, RNA:DNA hybrid and dsRNA helixes showed that dsDNA and RNA:DNA hybrid molecules have a similar conformation of their double-stranded helix with similar shapes of their minor and major groves. While there was an

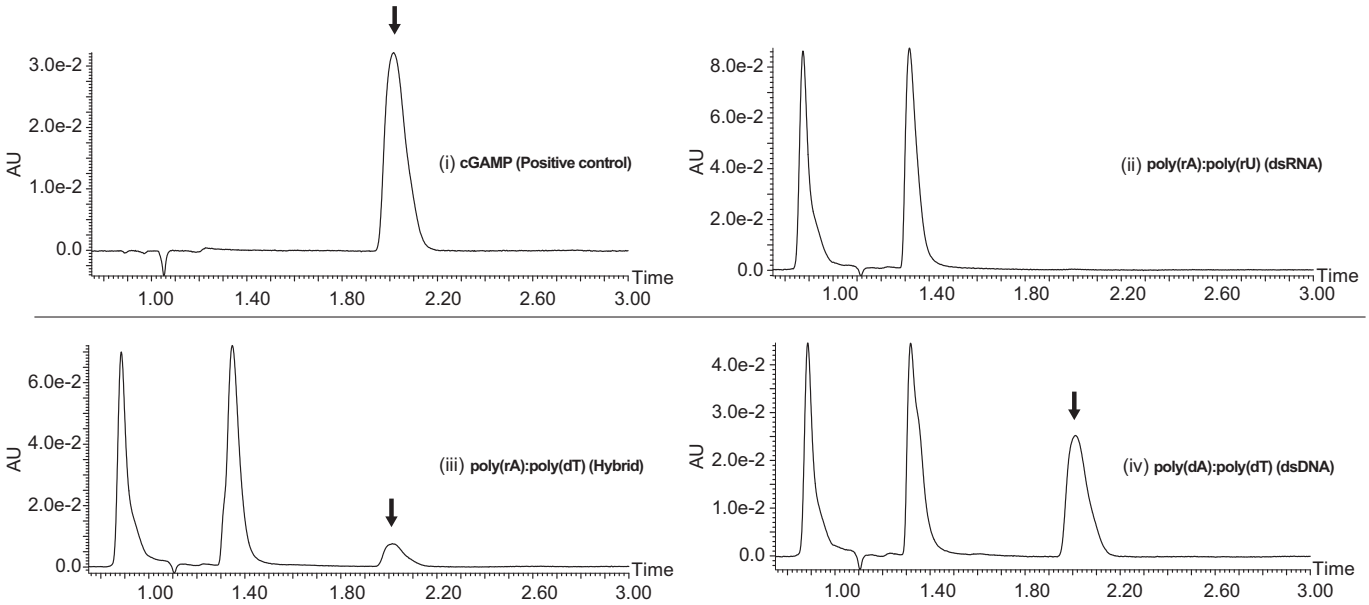

Figure 3. Recombinant cGAS protein synthesizes cGAMP(2′–5′) in the presence of poly(rA):poly(dT) hybrids.
RP-HPLC chromatograms showing the presence of cGAMP(2′–5′) after incubation of recombinant cGAS protein for 90 min in the presence of ATP and GTP with different ligands. (i) Synthetic 2′–5′ cGAMP as a positive control, (ii) poly(dA):poly(rU) dsRNA, (iii) poly(rA):poly(dT) hybrid and (iv) poly(dA):poly(dT) dsDNA.

obvious overlap between the orientation of the bases of RNA:DNA hybrids and dsDNA, the shape of a dsRNA helix differs from both the dsDNA and hybrid helices with the dsRNA helix being wider (Fig 5E and F). It is likely that this prevents its proper binding into the cGAS cleft and as such the conformational switch of cGAS that is required for its nucleotidyltransferase activity. As RNA:DNA hybrids can bind to cGAS in both orientations of the RNA chain, its binding to cGAS should lead to the same switch-like conformational changes of the activation loop, which are induced by dsDNA binding (Zhang *et al*, 2014) (Supplementary Fig S5). Altogether, these data proved that RNA:DNA hybrids can serve as ligands initiating cGAS activity.

Discussion

The presence of foreign nucleic acids or aberrant formation or translocation of self-nucleic acids triggers an immune response that is dependent on the interaction of these nucleic acids with different cytoplasmic PRRs. While the receptors and the subsequent pathways activated by intracellular dsDNA and dsRNA have been clearly ascertained, it was not established whether cytosolic RNA:DNA hybrids can also initiate immune responses. Here, we report that cytoplasmic RNA:DNA hybrids can indeed induce potent antiviral immune responses. Furthermore, we can ascribe the immunostimulatory activity of this ligand to the direct activation of the recently established dsDNA sensor cGAS.

To address the immunostimulatory activity RNA:DNA hybrids in the first place, it was important to obtain hybrids devoid of dsDNA contamination. A critical confounding factor present when generating RNA:DNA hybrids using reverse transcriptase is the synthesis of dsDNA from the first strand cDNA (Hsieh *et al*, 1993). To check for this possibility, we digested our *in vitro* transcribed hybrid samples with RNase H; however, we still observed some residual activation suggesting the presence of dsDNA. Consequently, we decided to use enzymatically generated long polynucleotides that could be annealed to form RNA:DNA hybrids. Of course, there is no biological correlate for this artificial duplex molecule; however, we consider it a sound model ligand, given the fact that ligand receptor interactions of double-stranded nucleic acids usually occur independent of their nucleobase composition, but are rather dependent on their tertiary structure.

Our *in vitro* studies using recombinant cGAS in conjunction with different nucleic acids show that the amount of cGAMP produced in response to the hybrids is not within the same range as observed with dsDNA. We hypothesize that this could be due to suboptimal activation of cGAS resulting from an inefficient conformational switch that is required for its enzyme activity. However, in a situation in which multiple signals are integrated by the cell (e.g. IP-10 production), low levels of cGAMP production might be sufficient to reach activity levels that are comparable to dsDNA stimulation. Interestingly, in some cases, we also observed an enhanced IFN response to single-stranded poly(dT) molecule while no such response was observed for poly(rA). However, at the same time, our *in vitro* data clearly demonstrate that poly(dT) by itself cannot activate cGAS. As such, we consider it likely that this weak, but consistent cGAS activation by poly(dT) *in vivo* is due to the intracellular formation of a cGAS stimulatory ligand (Supplementary Fig S6). While this phenomenon might not directly involve poly(dT) as a ligand, we speculate that poly(dT) can form DNA:RNA hybrids with endogenous poly(rA) in the context of mRNA tails.

Aberrant activation of the immune system in response to self-nucleic acids forms the basis for several chronic inflammatory

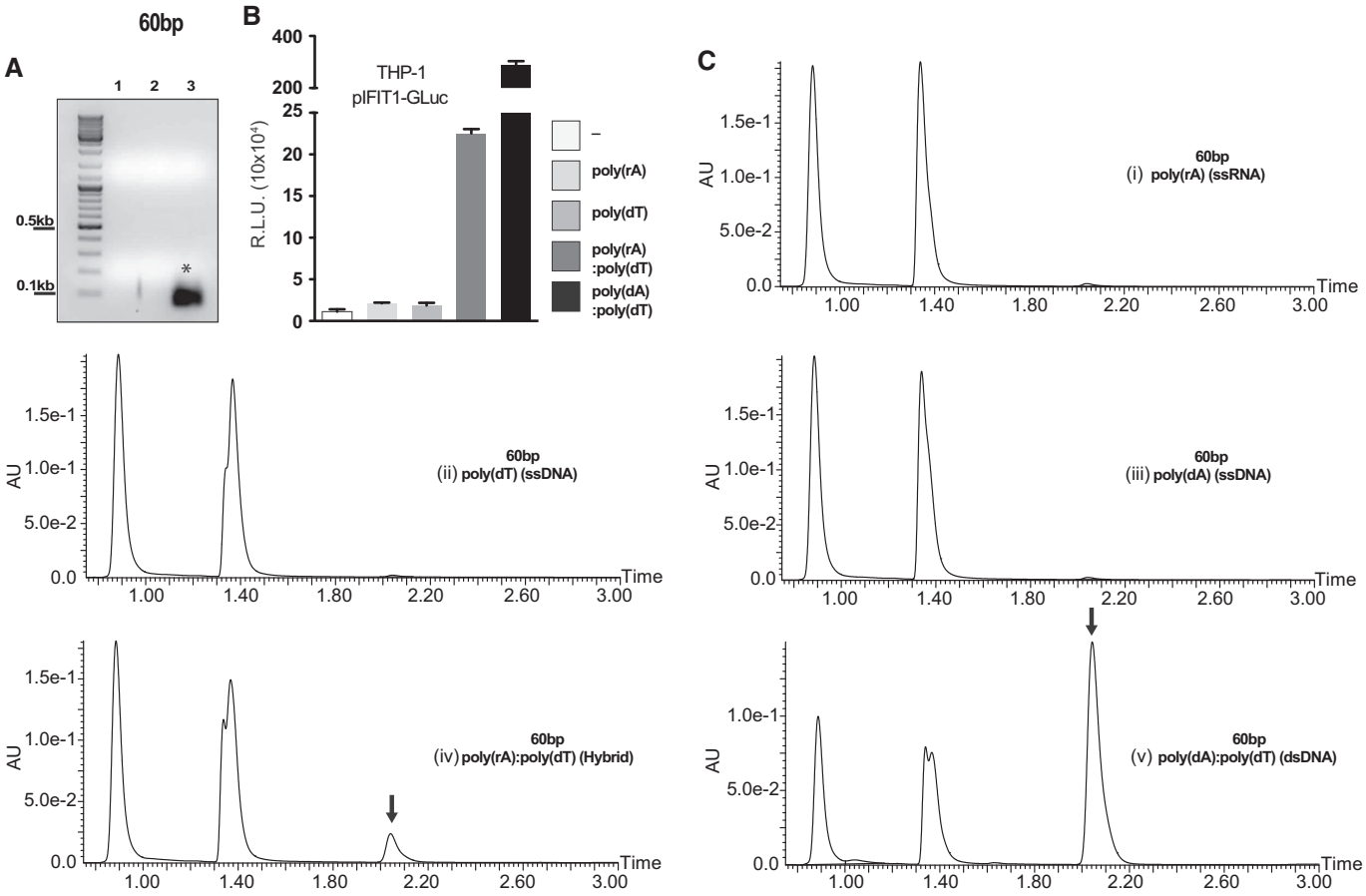

Figure 4. Recombinant cGAS protein synthesizes cGAMP(2′–5′) in the presence of 60-bp synthetic poly(rA):poly(dT) hybrids.

A 60-bp synthetic poly(rA) (lane 1) and 60-bp poly(dT) (lane 2) oligos were annealed, and the samples were run on a 1% agarose gel. Asterisk indicates annealed poly(rA):poly(dT) RNA:DNA hybrid (lane 3).

B Differentiated human monocyte THP-1 cells with Gaussia luciferase knockin under *IFIT1* promoter were transfected with or without 60-bp poly(rA), 60-bp poly(dT) or 60-bp poly(rA):poly(dT) (hybrid) and 60-bp poly(dA):poly(dT) (dsDNA) and luciferase assay was performed. Data shown are from two biological replicates. Data plot shows mean with SEM.

C RP-HPLC chromatograms showing the presence of cGAMP(2′–5′) after incubation of recombinant cGAS protein for 180 min in the presence of ATP and GTP with: (i) 60-bp poly(rA) (ssRNA), (ii) 60-bp poly(dT) (ssDNA), (iii) 60-bp poly(dA) (ssDNA), (iv) 60-bp poly(rA):poly(dT) (hybrid), or (v) 60-bp poly(dA):poly(dT) (dsDNA). Arrow indicates the expected peak for cGAMP (2′–5′), the product of cGAS catalyzed reaction.

diseases. Aicardi–Goutières syndrome (AGS), for example, is a rare but generally fatal condition associated with increased type I interferon production in the serum of respective patients. This condition can result from mutations in genes encoding for the nucleic acid metabolizing enzymes SAMHD1, TREX1, Ribonuclease H2 (RNASE H2A, RNASE H2B, RNASE H2C) or ADAR1 (La Piana *et al*, 2014; Lee-Kirsch *et al*, 2014). Even though it is quite conceivable that AGS-related mutations lead to the activation of cytosolic nucleic acid sensing pathways, this has only been documented for TREX1 deficiency. Here, it has been shown *in vivo* that the fatal consequences of TREX1 deficiency can be rescued by the deletion of STING, and *in vitro* studies have revealed that this is fully attributable to the activation of cGAS (Gall *et al*, 2012; Ablasser *et al*, 2014). However, the exact nature of the ligand that activates cGAS in this context still remains unclear. Interestingly, TREX1 has been shown to metabolize the reverse-transcribed DNA, and the absence of TREX1 resulted in the accumulation of DNA from endogenous retro elements (Stetson, 2012). On the other hand, the ribonuclease H2 enzyme complex is involved in the removal of the Okazaki fragments as well as aberrantly introduced ribonucleotides during the replication of the genome (Reijns *et al*, 2012). As such, the hypomorphic mutations in RNase H2 proteins, observed in AGS, could result in less efficient removal of the RNA strand or the incorporated ribonucleotides, thereby culminating in the accumulation of RNA:DNA hybrids. Unfortunately, the *Rnaseh2b* knockout mouse model does not display the expected phenotype of type I IFN-driven immune activation, which might be due to the fact that this condition does not lead to a cell-autonomous activation of nucleic acid sensing PRRs. A secondary activation of immune cells in the context of RNase H2 deficiency might, however, not be evident due to early embryonic lethality of these mice (Hiller *et al*, 2012; Reijns *et al*, 2012). As such, it would be worth revisiting this model with regard to identifying the culprit stimulatory ligand using conditionally ablated *Rnaseh2b*.

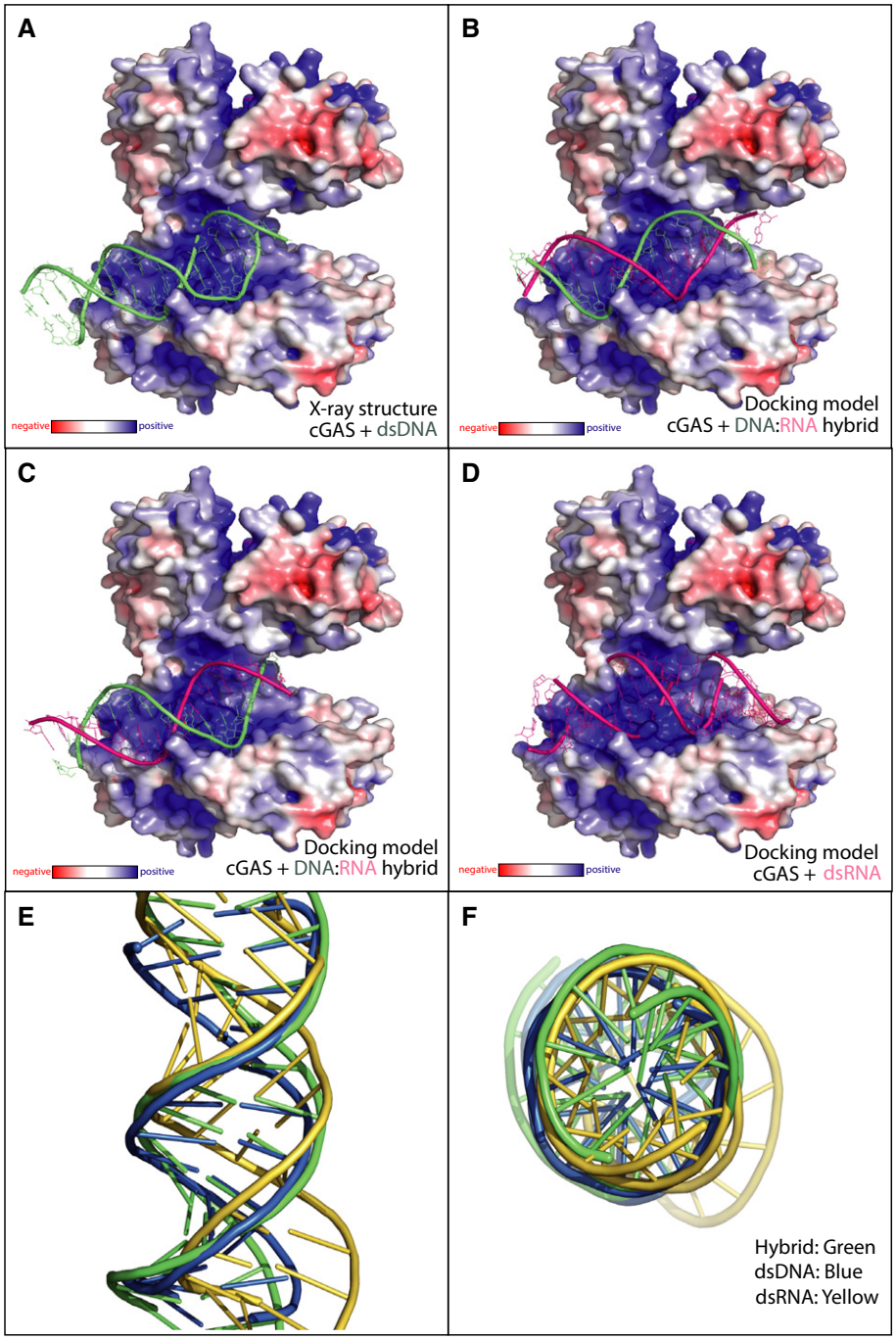

Figure 5. Modeling of dsDNA, RNA:DNA hybrids and dsRNA interaction with cGAS.

A–D HADDOCK models of different double-stranded nucleic acids in the crystal structure of pig cGAS are shown (the cGAS structure is based on the cGAS:dsDNA PDB ID 4KB6). The DNA strand is shown in green, whereas the RNA strand is depicted in pink. (A) dsDNA bound to cGAS (PDB ID 4KB6). (B, C) Best docking results of an RNA:DNA hybrid in two different orientations (PDB ID 4KB6 chain A) into cGAS are depicted. Hybrid molecules have been located in the cleft formed by the Zn-thumb and Arg150 of cGAS. (D) The best docking solution of dsRNA into the dsDNA binding region of cGAS.

E, F Cartoon and surface representation of superposition of dsDNA (blue), DNA:RNA hybrid (green) and dsRNA (yellow) molecules based on published structures.

Retroviruses could provide another source of intracellular RNA:DNA hybrids, which are generated by reverse transcriptase in the course of their replicative cycle (Telesnitsky & Goff, 1997). In this context, it was recently shown that viral-derived RNA:DNA hybrids accumulate in the cytoplasm and endosomal compartments of retrovirus (MMLV)-infected fibroblasts (Rigby *et al*, 2014). In the same study, the authors used synthetic 45- and 60-bp RNA:DNA hybrid molecules as stimuli and observed that while the response to the 45-bp hybrid molecule was completely TLR9 dependent, it was only partially dependent in the case of 60-bp hybrids. As such, to

account for the partial response still observed in the 60-bp hybrid-stimulated cells, the authors alluded to the existence of other cytoplasmic hybrid sensors. Given the restricted expression of TLR9 in the human system, we speculate that RNA:DNA hybrid detection by cGAS could constitute the predominant sensing mechanism in the human system. Indeed, the fact that retroviral infection has been shown to trigger proinflammatory gene expression in cells other than pDCs indicates the existence of additional cytoplasmic receptors for retroviral infection (Luban, 2012). In this regard, under permissive conditions, cGAS has been identified as the key intracellular sensor essential for mounting an antiviral response in the course of HIV infection in various cell types, including fibroblasts, myeloid dendritic cells and macrophages (Gao *et al*, 2013a). Here, it was demonstrated that inhibition of viral reverse transcriptase but not of viral integrase resulted in significant inhibition of IFN-β production. Unfortunately, this set of experiments cannot distinguish between the presence of RNA:DNA hybrids versus dsDNA as there is currently no technical means to differentially influence the formation of such nucleic acids during *in vivo* infections. Consequently, further studies will be required to identify the cGAS-stimulatory nucleic acid in the context of retroviral infection.

Interestingly, the presence of RNA:DNA hybrids has also been described in the life cycle of a number of DNA viruses, including herpesviridae (Prichard *et al*, 1998; Rennekamp & Lieberman, 2011) and hepadnaviruses (Summers & Mason, 1982; Miller *et al*, 1984). Moreover, mitochondrial nucleic acids, which have previously been described as DAMP molecules (Oka *et al*, 2012), harbor stable RNA:DNA hybrid structures that arise in the course of mtDNA replication (Yasukawa *et al*, 2006). Again, additional studies will be needed to decipher the possible contribution of RNA:DNA hybrids to the immunostimulatory capacities of these infectious or sterile inflammatory conditions.

In conclusion, we demonstrate that the intracellular presence of RNA:DNA hybrids elicits cGAS-dependent antiviral immune responses. Future studies will be required to identify the biological context of this sensing modality, yet as outlined above, we hypothesize that this mechanism could be of relevance in the context of aberrant recognition of endogenous nucleic acids or viral infections.

Materials and Methods

Generation of RNA:DNA hybrids

Equal amounts of synthetic poly(dT) (Sigma #P6905) and poly(rA) (Sigma # P9403) were mixed in 5× annealing buffer (50 mM Tris–HCl pH 7,6, 250 mM NaCl, 5 mM EDTA), for example, 40 μl poly (rA) (300 ng/μl) + 40 μl poly(dT) (300 ng/μl) in 20 μl 5× annealing buffer. The samples were incubated in a PCR block starting at 95°C with decreasing gradient of −1°C per 100 seconds until 20°C. 60-bp poly(rA) was purchased from Biomers. 60-bp poly(dA) and 60-bp poly(dT) were purchased from Integrated DNA Technologies.

Dot-blot for hybrids

Nitrocellulose membrane was marked and spotted with the RNA:DNA hybrids or poly(dA:dT) (dsDNA) as a negative control. The membrane was allowed to air dry for 2 h and then blocked in 0.5% milk in PBST buffer. The membrane was then incubated with the anti-hybrid S9.6 antibody overnight at 4°C, washed and probed with anti-mouse secondary antibody.

Cell culture

Murine BMDMs were isolated and cultured as per standard protocols. THP-1 cells were maintained in RPMI medium. The cells were differentiated for 3 h with PMA (330 ng/ml), the medium was removed, and the cells were washed with 1× PBS three times. The cells were detached in PBS, and 7×10^4 cells were plated in 96-well flat-bottomed plate. Isolation of PBMC from buffy coat was performed using standard protocol.

Stimulation with RNA:DNA hybrids

7×10^4 cells were incubated overnight in flat-bottomed 96-well plate. A transfection mix with Lipofectamine and 1 μg/ml of poly (rA), poly(dT), poly(rA):poly(dT) was prepared as per standard protocol. The cells were incubated with the nucleic acids overnight. The supernatants were collected and subjected to further assays. For RT–PCR, the cells were stimulated with the nucleic acids for 6 h.

RNase H, RNase A and DNase I digestion

1 μg of hybrid was digested with 1 μl of the RNase H, RNase A or DNase I (Fermentas) enzyme in a final reaction volume of 10 μl. The sample was incubated at 37°C for 30 min. The enzyme was heat-inactivated by incubating the samples at 65°C for 10 min, and the efficiency of digestion was checked by running the samples in 0.8% agarose gel.

RNA analysis

RNA isolation was performed using the QIAcube system (Qiagen), and equal amounts of RNA were used for cDNA synthesis. Real-time PCR analysis with Eva Green PCR Master Mix (Biobudget) was performed on Real-time PCR system (Roche). The expression of target genes was normalized to HPRT or GAPDH expression and plotted as arbitrary units on a linear scale. Primer sequences are available on request.

ELISA

Cell culture supernatants were assayed for human IP-10 and human IL-6 (BD Biosciences) according to the manufacturer's instructions.

STING, *MAVS* and *cGAS* KO THP-1 cells

THP-1 knockout cells were generated using the CRISPR/Cas9 system. A plasmid containing mCherry Cas9 and a U6 promoter-driven gRNA against STING, MAVS or cGAS was electroporated into THP-1 cells under following conditions: 5 μg plasmid were mixed with 250 μl cell suspension (10×10^6/ml in OptiMEM) and electroporated at 950 μF and 250 V. Cells were FACS sorted for mCherry expression 24 h after electroporation. Positive cells were

diluted under limiting conditions and plated in 96-well plates to obtain single cell clones. The genotype of THP-1 clones was analyzed by deep sequencing (Illumina, MiSeq) (Schmid-Burgk *et al*, 2014).

Generation of pIFIT1-GLuc THP-1 reporter cell line

To study induction of interferon-stimulated genes at the natural gene expression level using a reporter system, we generated a IFIT1 reporter cell line. Using the CRISPR/Cas9 system, the Gaussia luciferase gene was knocked into the *IFIT1* gene locus in THP-1 cells. For this purpose, a reporter insert cassette, harboring flanking 50-bp homology arms, a 2A peptide and the luciferase gene, was synthesized by a two-step PCR. THP-1 cells were co-electroporated with a CRISPR targeting the *IFIT1* locus and the Gaussia luciferase insert cassette. As the CRISPR construct contained a mCherry gene, electroporated cells were sorted for mCherry expression by FACS 24 h after electroporation. For isolation of reporter cell clones, cells were seeded under limiting dilution conditions. Single cell clones were tested for knockin of the luciferase gene by stimulation with synthetic triphosphate RNA (pppRNA) and subsequent measurement of luciferase induction. Positive reporter clones were validated by sequencing of the insert locus.

In vitro assay for cGAS activity

For *in vitro* reactions of cGAS in the presence of varying nucleic acids, 2 mM recombinant cGAS was mixed with 0.2 μg/μl poly(rA):poly(dT), poly(dA):poly(dT), poly(rA):poly(rU) or the corresponding single-stranded controls and 0.1 M ATP and 0.1 mM GTP in buffer A (100 mM NaCl, 40 mM Tris pH 7.5, 10 mM $MgCl_2$). After 45, 90 or 180 min of incubation at 37°C, the reaction mixture was analyzed by RP-HPLC. Samples were prepared in 0.3 M triethylammonium acetate, applied to a Waters XBridge C18 column (4.6 × 50 mm, 2.5 μm particle size) and separated in an isocratic gradient of 100 mM ammonium acetate for 5 min at a flow rate of 1 ml/min. Chemically synthesized cGAMP(2′–5′) (Ablasser *et al*, 2013a) served as a positive control.

Modeling of cGAS dsDNA, DNA:RNA hybrid and dsRNA complexes

Complexes of cGAS with three short double-stranded nucleic acids (NA) were modeled by docking of corresponding NA (dsDNA (PDB ID 4KB6) (Civril *et al*, 2013) or (PDB ID 3V6T) (Deng *et al*, 2012), DNA:RNA hybrid (PDB ID 4GG4) (Yin *et al*, 2012) and dsRNA (PDB ID 3KS8) (Kimberlin *et al*, 2010) into the structure of pig cGAS (PDB ID 4KB6 chain A) (Civril *et al*, 2013)). Docking was done on the HADDOCK server (de Vries *et al*, 2010). HADDOCK permits position restrained docking of NA into proteins. Sets of residues for docking in cGAS and dsDNA that should interact with NA have been taken from the original crystal structure of the cGAS–dsDNA complex (PDB ID 4KB6) (Civril *et al*, 2013). Visualization of the results was performed using PyMol.

Statistics

Statistical tests were performed using GraphPad Prism program. For column statistics, one-way ANOVA with Bonferroni's or Tukey's multiple comparison test was performed. $P \leq 0.05$ was considered significant.

Supplementary information for this article is available online: http://emboj.embopress.org

Acknowledgements

The authors wish to thank Dr. Stephen Leppla, NIH/NIAID, USA for providing the anti-Hybrid S9.6 antibody and Jonathan Schmid-Burgk and Thomas Ebert (all University of Bonn, Bonn, Germany) for technical support. This work was supported by grants from the German Research Foundation (SFB704 and SFB670) and the European Research Council (ERC-2009-StG 243046) to VH. VH is a member of the excellence cluster ImmunoSensation.

Author contributions

AKM and VH planned the experiments. AKM, TS, DC and MG performed the experiments. KH and MG generated the pIFIT1-GLuc THP-1 cells. LA purified recombinant cGAS. K-PH and AVK performed the *in silico* structural analysis. AKM and VH drafted the manuscript.

Conflict of interest

The authors declare that they have no conflict of interest.

References

Ablasser A, Goldeck M, Cavlar T, Deimling T, Witte G, Rohl I, Hopfner KP, Ludwig J, Hornung V (2013a) cGAS produces a 2′–5′-linked cyclic dinucleotide second messenger that activates STING. *Nature* 498: 380 – 384

Ablasser A, Hertrich C, Wassermann R, Hornung V (2013b) Nucleic acid driven sterile inflammation. *Clin Immunol* 147: 207 – 215

Ablasser A, Schmid-Burgk JL, Hemmerling I, Horvath GL, Schmidt T, Latz E, Hornung V (2013c) Cell intrinsic immunity spreads to bystander cells via the intercellular transfer of cGAMP. *Nature* 503: 530 – 534

Ablasser A, Hemmerling I, Schmid-Burgk JL, Behrendt R, Roers A, Hornung V (2014) TREX1 deficiency triggers cell-autonomous immunity in a cGAS-dependent manner. *J Immunol* 192: 5993 – 5997

Barbalat R, Ewald SE, Mouchess ML, Barton GM (2011) Nucleic acid recognition by the innate immune system. *Annu Rev Immunol* 29: 185 – 214

Boguslawski SJ, Smith DE, Michalak MA, Mickelson KE, Yehle CO, Patterson WL, Carrico RJ (1986) Characterization of monoclonal antibody to DNA.RNA and its application to immunodetection of hybrids. *J Immunol Methods* 89: 123 – 130

Civril F, Deimling T, de Oliveira Mann CC, Ablasser A, Moldt M, Witte G, Hornung V, Hopfner KP (2013) Structural mechanism of cytosolic DNA sensing by cGAS. *Nature* 498: 332 – 337

Crow YJ (2011) Type I interferonopathies: a novel set of inborn errors of immunity. *Ann N Y Acad Sci* 1238: 91 – 98

de Vries SJ, van Dijk M, Bonvin AM (2010) The HADDOCK web server for data-driven biomolecular docking. *Nat Protoc* 5: 883 – 897

Deng D, Yan C, Pan X, Mahfouz M, Wang J, Zhu JK, Shi Y, Yan N (2012) Structural basis for sequence-specific recognition of DNA by TAL effectors. *Science* 335: 720 – 723

Diner EJ, Burdette DL, Wilson SC, Monroe KM, Kellenberger CA, Hyodo M, Hayakawa Y, Hammond MC, Vance RE (2013) The innate immune DNA sensor cGAS produces a noncanonical cyclic dinucleotide that activates human STING. *Cell Rep* 3: 1355 – 1361

Gall A, Treuting P, Elkon KB, Loo YM, Gale M Jr, Barber GN, Stetson DB (2012) Autoimmunity initiates in nonhematopoietic cells and progresses via lymphocytes in an interferon-dependent autoimmune disease. *Immunity* 36: 120 – 131

Gao D, Wu J, Wu YT, Du F, Aroh C, Yan N, Sun L, Chen ZJ (2013a) Cyclic GMP-AMP synthase is an innate immune sensor of HIV and other retroviruses. *Science* 341: 903 – 906

Gao P, Ascano M, Wu Y, Barchet W, Gaffney BL, Zillinger T, Serganov AA, Liu Y, Jones RA, Hartmann G, Tuschl T, Patel DJ (2013b) Cyclic [G(2′,5′)pA(3′,5′)p] is the metazoan second messenger produced by DNA-activated cyclic GMP-AMP synthase. *Cell* 153: 1094 – 1107

Goubau D, Deddouche S, Reis e Sousa C (2013) Cytosolic sensing of viruses. *Immunity* 38: 855 – 869

Hiller B, Achleitner M, Glage S, Naumann R, Behrendt R, Roers A (2012) Mammalian RNase H2 removes ribonucleotides from DNA to maintain genome integrity. *J Exp Med* 209: 1419 – 1426

Hsieh JC, Zinnen S, Modrich P (1993) Kinetic mechanism of the DNA-dependent DNA polymerase activity of human immunodeficiency virus reverse transcriptase. *J Biol Chem* 268: 24607 – 24613

Hu Z, Zhang A, Storz G, Gottesman S, Leppla SH (2006) An antibody-based microarray assay for small RNA detection. *Nucleic Acids Res* 34: e52

Kimberlin CR, Bornholdt ZA, Li S, Woods VL Jr, MacRae IJ, Saphire EO (2010) Ebolavirus VP35 uses a bimodal strategy to bind dsRNA for innate immune suppression. *Proc Natl Acad Sci USA* 107: 314 – 319

La Piana R, Uggetti C, Olivieri I, Tonduti D, Balottin U, Fazzi E, Orcesi S (2014) Bilateral striatal necrosis in two subjects with Aicardi-Goutieres syndrome due to mutations in ADAR1 (AGS6). *Am J Med Genet A* 164: 815 – 819

Lee-Kirsch MA, Wolf C, Gunther C (2014) Aicardi-Goutieres syndrome: a model disease for systemic autoimmunity. *Clin Exp Immunol* 175: 17 – 24

Luban J (2012) Innate immune sensing of HIV-1 by dendritic cells. *Cell Host Microbe* 12: 408 – 418

Medzhitov R (2007) Recognition of microorganisms and activation of the immune response. *Nature* 449: 819 – 826

Miller RH, Tran CT, Robinson WS (1984) Hepatitis B virus particles of plasma and liver contain viral DNA-RNA hybrid molecules. *Virology* 139: 53 – 63

Oka T, Hikoso S, Yamaguchi O, Taneike M, Takeda T, Tamai T, Oyabu J, Murakawa T, Nakayama H, Nishida K, Akira S, Yamamoto A, Komuro I, Otsu K (2012) Mitochondrial DNA that escapes from autophagy causes inflammation and heart failure. *Nature* 485: 251 – 255

Prichard MN, Jairath S, Penfold ME, St Jeor S, Bohlman MC, Pari GS (1998) Identification of persistent RNA-DNA hybrid structures within the origin of replication of human cytomegalovirus. *J Virol* 72: 6997 – 7004

Reijns MA, Rabe B, Rigby RE, Mill P, Astell KR, Lettice LA, Boyle S, Leitch A, Keighren M, Kilanowski F, Devenney PS, Sexton D, Grimes G, Holt IJ, Hill RE, Taylor MS, Lawson KA, Dorin JR, Jackson AP (2012) Enzymatic removal of ribonucleotides from DNA is essential for mammalian genome integrity and development. *Cell* 149: 1008 – 1022

Rennekamp AJ, Lieberman PM (2011) Initiation of Epstein-Barr virus lytic replication requires transcription and the formation of a stable RNA-DNA hybrid molecule at OriLyt. *J Virol* 85: 2837 – 2850

Rigby RE, Webb LM, Mackenzie KJ, Li Y, Leitch A, Reijns MA, Lundie RJ, Revuelta A, Davidson DJ, Diebold S, Modis Y, Macdonald AS, Jackson AP (2014) RNA:DNA hybrids are a novel molecular pattern sensed by TLR9. *EMBO J* 33: 542 – 558

Schmid-Burgk JL, Schmidt T, Gaidt MM, Pelka K, Latz E, Ebert TS, Hornung V (2014) OutKnocker: a web tool for rapid and simple genotyping of designer nuclease edited cell lines. *Genome Res* 24: 1719 – 1723

Stetson DB (2012) Endogenous retroelements and autoimmune disease. *Curr Opin Immunol* 24: 692 – 697

Summers J, Mason WS (1982) Replication of the genome of a hepatitis B–like virus by reverse transcription of an RNA intermediate. *Cell* 29: 403 – 415

Sun L, Wu J, Du F, Chen X, Chen ZJ (2013) Cyclic GMP-AMP synthase is a cytosolic DNA sensor that activates the type I interferon pathway. *Science* 339: 786 – 791

Telesnitsky A, Goff SP (1997) Reverse transcriptase and the generation of retroviral DNA. In *Retroviruses*, Coffin JM, Hughes SH, Varmus HE (eds). Cold Spring Harbor, NY: Cold Spring Harbor Laboratory Press.

Wu J, Sun L, Chen X, Du F, Shi H, Chen C, Chen ZJ (2013) Cyclic GMP-AMP is an endogenous second messenger in innate immune signaling by cytosolic DNA. *Science* 339: 826 – 830

Yasukawa T, Reyes A, Cluett TJ, Yang MY, Bowmaker M, Jacobs HT, Holt IJ (2006) Replication of vertebrate mitochondrial DNA entails transient ribonucleotide incorporation throughout the lagging strand. *EMBO J* 25: 5358 – 5371

Yin P, Deng D, Yan C, Pan X, Xi JJ, Yan N, Shi Y (2012) Specific DNA-RNA hybrid recognition by TAL effectors. *Cell Rep* 2: 707 – 713

Zhang X, Shi H, Wu J, Sun L, Chen C, Chen ZJ (2013) Cyclic GMP-AMP containing mixed phosphodiester linkages is an endogenous high-affinity ligand for STING. *Mol Cell* 51: 226 – 235

Zhang X, Wu J, Du F, Xu H, Sun L, Chen Z, Brautigam CA, Chen ZJ (2014) The cytosolic DNA sensor cGAS forms an oligomeric complex with DNA and undergoes switch-like conformational changes in the activation loop. *Cell Rep* 6: 421 – 430

